J. Phys. C: Solid State Phys., Vol. 9, 1976. Printed in Great Britain. © 1976

Static and dynamic interactions with spatially dispersive media

Derek Chan† and Peter Richmond
Unilever Research Port Sunlight Laboratory, Port Sunlight, Wirral, Merseyside, L62 4XN, UK

Received 28 August 1975

Abstract. We have evaluated the dynamical image interaction between a moving charge and a spatially dispersive medium as well as the Van der Waals dispersion energy between a dipole and the same substrate. The spatially dispersive medium is represented by the 'infinite barrier' model with specular reflection of current fluctuations at the interface. Numerical estimates of the effect are computed using a hydrodynamic model for the dielectric permittivity.

1. Introduction

In a series of papers we have considered the effects of spatial dispersion on the Lifshitz–van der Waals interaction between macroscopic bodies (Chan and Richmond 1975a, b—to be referred to as I and II). Our derivation in terms of a general wavevector-dependent bulk dielectric permittivity $\epsilon(\boldsymbol{q}, \omega)$ was based on the so-called 'infinite barrier' model. That is, we supposed that the charge carriers were reflected specularly at the interfaces. Similar results have recently been derived independently by Inglesfield and Wikborg (1975) and Harris and Griffin (1975).

Now calculations which include retardation effects for interacting metal bodies across air indicate that the effect of spatial dispersion may be quite significant (Chan and Richmond 1976). However, the distances at which this effect occurs are not large ($\lesssim 30$ Å) and although it may be possible to observe the effect using particle removal experiments such as have been done in colloid science (Visser 1973) these are likely to be difficult. Another way may be via physisorption experiments such as measurements of the isosteric heats of adsorption which are related directly to the interaction potential between the atom and substrate. For example, using a simple Lifshitz–van der Waals potential combined with a fixed cut-off distance we have recently correlated the isosteric heats for homologous series of hydrocarbons and alcohols on graphite (Chan and Richmond 1975c). Clearly similar experiments may be done on metals.

A complete theoretical analysis of this situation should strictly include a treatment of the overlap of the electron wavefunctions. However, an analysis of the Lifshitz–van der Waals interaction using the infinite barrier model may give a useful estimate of the physisorption potential for certain atoms. This combined with a cut-off in the manner suggested above may then yield isosteric heats.

† CSIRO Post-Doctoral Research Fellow.

Another way of studying spatial dispersion may be via electron scattering techniques. Thus it is also of interest to calculate the effect of spatial dispersion on the dynamical image interaction of a charged particle moving with respect to a substrate. The dynamical image interaction of charges with dielectrics has been studied by a number of authors (Ray and Mahan 1972, Takimoto 1966, Ritchie 1957). We have shown elsewhere how classical techniques may be used to calculate this interaction (Chan and Richmond 1973).

In this note we compute both the static interaction between a dipole and spatially dispersive substrate as well as the dynamical interaction between a charge and the same substrate.

2. Dynamical image interaction

Consider a charge of strength Q with velocity $\boldsymbol{v}$ moving with respect to a planar spatially dispersive substrate with bulk dielectric permittivity $\epsilon(\boldsymbol{q};\omega)$. We suppose the charge may not penetrate the surface but is reflected at time $t = 0$. Choosing a co-ordinate system with z axis perpendicular to the plane substrate which occupies the half space $z < 0$ we may write the charge density of the moving particle $\bar{\rho}(r, t) = Q\delta(x)\delta(y - v_{\parallel}t)$ $\delta(z - v_{\perp}|t|)$ where $v_{\parallel}$ is the component of the velocity parallel to the surface (y axis) and $v_{\perp}$ is the magnitude of the z component.

We now introduce the two-dimensional Fourier transform of the electric potential Φ:

$$\Phi(\boldsymbol{r}, t) = \int \frac{d^2\boldsymbol{K}}{(2\pi)^2} \int_{-\infty}^{\infty} \frac{d\omega}{2\pi} \exp\left[i(\boldsymbol{K}\,.\,\boldsymbol{\sigma} - \omega t)\right]\phi(\boldsymbol{K}; z; \omega) \tag{1}$$

where $\boldsymbol{\sigma}$ and $\boldsymbol{K}$ are two-dimensional vectors: $\boldsymbol{\sigma} = (x, y)$ and $\boldsymbol{K} = (K_x, K_y)$. Following our earlier work (references I and II) we may write:

$$\phi(z; \boldsymbol{K}, \omega) = \int_{-\infty}^{\infty} \frac{dk}{2\pi} \frac{e^{ikz}}{k^2 + K^2} 4\pi\{A(\boldsymbol{K}, \omega) + \rho(\boldsymbol{q}; \omega)\} \qquad z > 0 \tag{2}$$

$$\phi(z; \boldsymbol{K}, \omega) = \int_{-\infty}^{\infty} \frac{dk}{2\pi} \frac{e^{ikz}}{(k^2 + K^2)\epsilon(\boldsymbol{q}, \omega)} 4\pi B(\boldsymbol{K}, \omega) \qquad z < 0 \tag{3}$$

where $\rho(\boldsymbol{q}, \omega)$ is the usual three-dimensional Fourier transform of the charge density given by:

$$\bar{\rho}(\boldsymbol{r}; t) = \int \frac{d^3q}{(2\pi)^3} \int \frac{d\omega}{2\pi} \exp\left[i(\boldsymbol{q}\,.\,\boldsymbol{r} - \omega t)\right]\rho(\boldsymbol{q}; \omega) \tag{4}$$

and

$$\rho(\boldsymbol{q}; \omega) = \int d\boldsymbol{r} \int dt \exp\left[-i(\boldsymbol{q}\,.\,\boldsymbol{r} - \omega t)\right]\bar{\rho}(\boldsymbol{r}; t)$$

$$= 2Q \int_{-\infty}^{\infty} dt \exp(-ik\, v_{\perp} t) \cos(\omega - K_y v_{\parallel})t. \tag{5}$$

The z components are of the displacement vector are

$$D^z(z; \boldsymbol{K}; \omega) = -\,\partial\phi/\partial z \qquad z > 0 \tag{6}$$

and

$$D^z(z; \boldsymbol{K}; \omega) = \int_{\infty}^{\gamma} \frac{dk}{2\pi} \frac{e^{ikz}(-ik)}{(k^2 + K^2)} 4\pi B(\boldsymbol{K}; \omega) \qquad z < 0. \tag{7}$$

Expressed in this form, the specular reflection of fluctuating currents at the surface of the spatially dispersive medium is automatically accounted for (note $\boldsymbol{q} = (\boldsymbol{K}, k)$).

Now after some elementary manipulations we obtain from (5):

$$4\pi \int_{-\infty}^{\infty} \frac{\mathrm{d}k}{2\pi} \frac{\mathrm{e}^{ikz}}{k^2 + K^2} \rho(\boldsymbol{q}, \omega) = \frac{4\pi Q}{k} \frac{K v_\perp}{(K v_\perp)^2 + (\omega - K_y v_\parallel)^2} \{2 \cos [(\omega - K_y v_\parallel) z / v_\perp] - \exp(-Kz)\}. \tag{8}$$

It is now a straightforward matter to match the usual boundary conditions across the interface at $z = 0$ to obtain:

$$A(\boldsymbol{k}, \omega) = -\left(\frac{\hat{\epsilon} - 1}{\hat{\epsilon} + 1}\right) \frac{2 Q v_\perp}{(K v_\perp)^2 + (\omega - K_y v_\parallel)^2} \tag{9}$$

where

$$\frac{1}{\hat{\epsilon}(\boldsymbol{K}, \omega)} = 2K \int_{-\infty}^{\infty} \frac{\mathrm{d}k}{2\pi} \frac{1}{q^2 \epsilon(\boldsymbol{q}, \omega)}. \tag{10}$$

The dynamical image interaction, V, is now given in terms of the induced potential in the region $z > 0$:

$$V = \tfrac{1}{2} \int \mathrm{d}^3 \boldsymbol{r} \bar{\rho}(\boldsymbol{r}, t) \Phi^{\mathrm{ind}}(\boldsymbol{r}, t) \tag{11}$$

where

$$\Phi^{\mathrm{ind}}(\boldsymbol{r}t) = \int \frac{\mathrm{d}^2 \boldsymbol{K}}{(2\pi)^2} \int \frac{\mathrm{d}\omega}{2\pi} \exp(\mathrm{i}\boldsymbol{K} \cdot \boldsymbol{\sigma} - \mathrm{i}\omega t) \int_{-\infty}^{\infty} \frac{\mathrm{d}k}{2\pi} \mathrm{e}^{ikz} \frac{4\pi A(\boldsymbol{K}; \omega)}{k^2 + K^2}. \tag{12}$$

From (9), (11) and (12) we immediately obtain:

$$V(z = v_\perp |t|) = -\frac{Q^2 v_\perp}{(2\pi)^2} \int \mathrm{d}^2 \boldsymbol{K} \int_{-\infty}^{\infty} \mathrm{d}\omega \exp[-i(\omega - K_y v_\parallel) t] \left(\frac{\hat{\epsilon} - 1}{\hat{\epsilon} + 1}\right) \frac{\mathrm{e}^{-Kz}}{(K v_\perp)^2 + (\omega - K_y v_\parallel)^2}. \tag{13}$$

For an incoming particle $t < 0$ the integral over ω may be done by closing the contour in the UHP. (Note that $\hat{\epsilon}$ is analytic in the UHP since it is a 'retarded' function.)

Thus we finally obtain:

$$V = \frac{-Q^2}{4\pi} \int \mathrm{d}^2 \boldsymbol{K} \frac{\mathrm{e}^{-2Kz}}{K} \left[\frac{\hat{\epsilon} - 1}{\hat{\epsilon} + 1}\right]_{\omega = K_y v_\parallel + \mathrm{i} K v_\perp}. \tag{14}$$

In order to proceed we use the well documented hydrodynamic model for the dielectric function, i.e.

$$\epsilon(\boldsymbol{q}, \omega) = 1 + \frac{\omega_\mathrm{p}^2}{\beta^2 q^2 - \omega^2} \tag{15}$$

in conjunction with the relation $\beta^2 = \frac{3}{5} V_\mathrm{F}^2$ where V_F is the Fermi velocity. This definition ensures the long-wavelength dispersion of the bulk plasmon mode agrees with that given by complete quantum mechanical calculations. Furthermore, we have considered only normal incidence, i.e. $v_\parallel = 0$. We now obtain for the interaction energy

$$V_\perp(z; v_\perp; \beta) = \frac{-Q^2}{2} \int_0^\infty \mathrm{d}K \, \mathrm{e}^{-2Kz} \frac{[1 + K^2(v_\perp^2 + \beta^2)/\omega_\mathrm{p}^2]^{1/2} - K\beta/\omega_\mathrm{p}}{(1 + 2K^2 v_\perp^2/\omega_\mathrm{p}^2)[1 + K^2(v_\perp^2 + \beta^2)/\omega_\mathrm{p}^2]^{1/2} + K\beta/\omega_\mathrm{p}} \tag{16}$$

Clearly as $z \to \infty$ the exponential dominates the integral and we may replace K by zero in the remainder to obtain the leading order

$$V_{\perp}(z) \sim \frac{-Q^2}{2} \int_0^{\infty} \mathrm{d}K\, \mathrm{e}^{-2Kz} \times 1 = -Q^2/4z \tag{17}$$

which is the usual Coulomb potential. However, for finite values of z, the present result deviates significantly from this potential. We have computed the dynamical image potential for the case of an aluminium substrate where $\hbar\omega_{\mathrm{p}} = 14{\cdot}2$ eV and the Fermi energy $E_{\mathrm{F}} = 11{\cdot}64$ eV. In figures 1*a–c* we have plotted the ratio (solid curves)

$$R(\beta, z) = V_{\perp}(z; v_{\perp}; \beta)/(-Q^2/4z)$$

and compared it with the local limit $R(0, z)$ (broken curves) to illustrate how spatial dispersion affects the dynamical image interaction. The results in figure 1*a–c* correspond to incident electrons of energy 1, 10, 100 eV respectively.

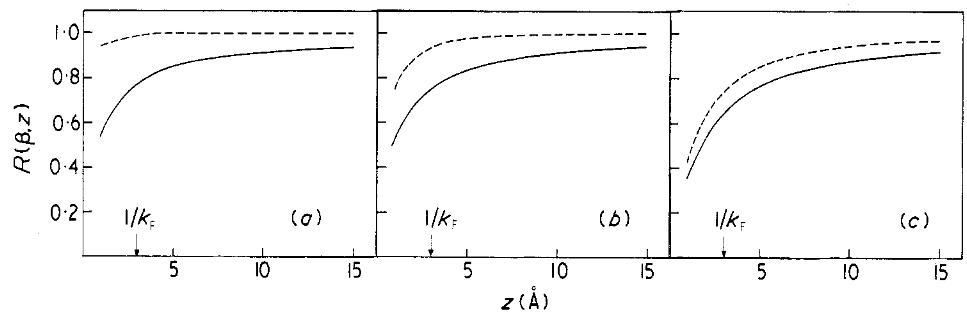

Figure 1. The ratio of the dynamical image interaction energy to the coulomb potential, $R(\beta, z)$ (see text), with (solid curves) and without (broken curve) spatial dispersion, as a function of distance (Å). The substrate is aluminium $\hbar\omega_{\mathrm{p}} = 14{\cdot}2$ eV, $E_{\mathrm{F}} = 11{\cdot}64$ eV. Figures *a–c* correspond to incident electrons of energy 1, 10, 100 eV respectively.

From the results we see that for fast electrons spatial dispersion is not important (figure 1*c*) since the electron only couples effectively with the high-frequency, long-wavelength surface excitations. For slow electrons, the short-wavelength response of the surface plasmon modifies significantly the dynamical image interaction (figure 1*a*). In this case the charges in the substrate have sufficient time to respond and screen out the interaction.

3. Van der Waals interaction

Consider now an oscillating dipole which for simplicity is assumed to have an isotropic polarizability $\alpha(\omega)$. The dipole is situated in air at $\boldsymbol{r}_1 = (\boldsymbol{\sigma}_1, z_1)$ $(z_1 > 0)$ above a planar semi-infinite spatially dispersive substrate occupying $z < 0$.

We may obtain the van der Waals interaction using the well known method of normal modes (van Kampen *et al* 1968). This may be obtained directly from the response to an oscillating test charge situated at $\boldsymbol{r}_1$ (Richmond 1974). Thus, using the same notation as above we have:

$$\phi = \begin{cases} \displaystyle\int_{-\infty}^{\infty} \frac{dk}{2\pi} \frac{e^{ikz}}{k^2 + K^2} 4\pi\{A(\boldsymbol{K}, \omega) + \rho(\boldsymbol{q}, \omega)\} & z > 0 \quad (18) \\ \displaystyle\int_{-\infty}^{\infty} \frac{dk}{2\pi} \frac{e^{ikz}}{k^2 + K^2} 4\pi B(\boldsymbol{K}, \omega) & z < 0 \quad (19) \end{cases}$$

where now we have:

$$\rho(\boldsymbol{q}, \omega) = \int d\boldsymbol{r} \exp(-i\boldsymbol{q} \cdot \boldsymbol{r})\bar{\rho}(\boldsymbol{r}, \omega) \tag{20}$$

and

$$\bar{\rho}(\boldsymbol{r}, \omega) = \delta(\boldsymbol{r} - \boldsymbol{r}_1)\, e^{i\omega t}. \tag{21}$$

The z component of the displacement vector is given by equations (6) and (7). Matching boundary conditions now yields the charge response function:

$$\Phi^{\text{ind}}(\boldsymbol{r}; \boldsymbol{r}_1; \omega) = -\int \frac{d^2\boldsymbol{K}}{2\pi^2} \exp[i\boldsymbol{K} \cdot (\boldsymbol{\sigma} - \boldsymbol{\sigma}_1)] \frac{4\pi}{2K}\left(\frac{\hat{\epsilon} - 1}{\hat{\epsilon} + 1}\right) \exp[-K(z + z_1)]. \tag{22}$$

The dipole response matrix $\mathbf{G}$ is now readily obtained. We have:

$$\mathbf{G}(\boldsymbol{r}; \omega) = -\lim_{\boldsymbol{r} \to \boldsymbol{r}_1} [\nabla_{\boldsymbol{r}}; \nabla_{\boldsymbol{r}_1} \Phi^{\text{ind}}(\boldsymbol{r}; \boldsymbol{r}_1; \omega)]. \tag{23}$$

Imposing self-consistency, i.e. $\boldsymbol{P} = \alpha\mathbf{G}\boldsymbol{P}$, now yields the required secular determinant:

$$D(\omega) = |\mathbf{1} - \alpha\mathbf{G}| \tag{24}$$

The van der Waals interaction between dipole and substrate is now

$$\begin{aligned} V_{\text{VDW}} &= k_B T \sum_{n=0}^{\infty}{}' \ln |\mathbf{1} - \alpha\mathbf{G}| \\ &\simeq -k_B T \sum_{n=0}^{\infty}{}' \operatorname{Tr}\{\mathbf{G}\}\alpha(i\xi_n). \end{aligned} \tag{25}$$

From equations (22), (23) and (25) we now finally obtain:

$$V_{\text{VDW}} = -2k_B T \sum_{n=0}^{\infty}{}' \alpha(i\xi_n) \int_0^{\infty} dK K^2 e^{-2Kz}\left(\frac{\hat{\epsilon} - 1}{\hat{\epsilon} + 1}\right). \tag{26}$$

For metals the dominant contribution comes from frequencies $\xi_n = 2\pi n k_B T/\hbar \sim \omega_p$ and we may replace the sum over frequencies by an integral using the prescription

$$k_B T \sum_{n=0}^{\infty}{}' \to \hbar/2\pi \int_0^{\infty} d\xi.$$

As before, in order to proceed we have used the hydrodynamic model for the dielectric function (equation 15) and a simple oscillator representation for the dipole, i.e.

$$\alpha(i\xi) = \alpha_0/(1 + \xi^2/\omega_0^2). \tag{27}$$

We now obtain from equation (26):

$$V_{\text{VDW}}(\beta; z) = -\frac{\hbar\omega_p\alpha_0}{8\pi z^3} \int_0^{\infty} \frac{dx}{1 + \gamma^2 x^2} \int_0^{\infty} dy\, y^2 e^{-y} \left[\frac{(1 + x^2 + \zeta^2 y^2)^{\frac{1}{2}} - \zeta y}{(1 + 2\zeta^2 y^2)(1 + x^2 + \zeta y^2)^{\frac{1}{2}} + \zeta y}\right] \tag{28}$$

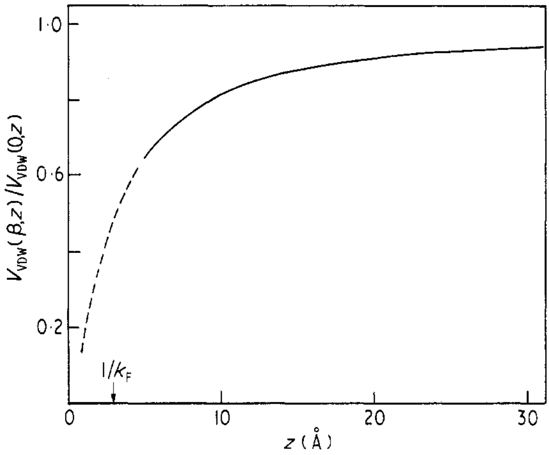

Figure 2. The ratio of the van der Waals potential with or without spatial dispersion for an isotropic dipole of characteristic frequency $\omega_0 = 2 \times 10^{16}$ rad s^{-1} as a function of distance (Å). Other data are the same as in figure 1. In the régime which is denoted by a broken line, our result becomes less accurate since the detailed nature of the interface becomes important.

where $\gamma = \omega_p/\omega_0$, $\zeta = \beta/2\omega_p z$. Clearly, in the limit $\beta = 0$, we obtain the normal van der Waals interaction $V_{VDW}(0; z) = -\hbar\omega_p\alpha_0\gamma/8z^3$. In figure 2 we have plotted $V_{VDW}(\beta; z)/V_{VDW}(0; z)$ for $\omega_0 = 2 \times 10^{16}$ rad s^{-1}, $\hbar\omega_p = 14{\cdot}2$ eV and $E_F = 11{\cdot}64$ eV. (Note that this ratio is independent of α_0.) The effects of spatial dispersion are clearly evident well before we expect the theory to break down $z \gtrsim k_F^{-1}$. This should then be reflected in the isosteric heat since it is essentially proportional to the minimum in the interaction potential, i.e. a calculation omitting spatial dispersion would give an over-estimate of the isosteric heat.

References

Chan D and Richmond P 1973 *Surface Sci.* **39** 437
—— 1975a *J. Phys.* C: *Solid St. Phys.* **8** 2509
—— 1975b *J. Phys.* C: *Solid St. Phys.* **8** 3221
—— 1975c *Discuss. Faraday Soc.* **59**
—— 1976 *J. Phys.* C: *Solid St. Phys.* **9** 149–58
Harris J and Griffin A 1975 *Phys. Rev.* **B11** 3669
Inglesfield J E and Wikborg E 1975 *Solid St. Commun.* **16** 335
Ray R and Mahan G D 1972 *Phys. Lett.* **21A** 301
Richmond P 1974 *J. Chem. Soc. Faraday Trans II* **70** 1650
Ritchie R H 1957 *Phys. Rev.* **106** 874
Takimoto N 1966 *Phys. Rev.* **146** 366
van Kampen N G, Nijboer B R A and Schram K 1968 *Phys. Lett.* **26A** 307
Visser J 1973 *PhD Thesis* Liverpool Polytechnic CNAA